



We certify that we have read the present work and that in our opinion it is fully adequate in scope and quality as a thesis towards the partial fulfillment of the Master's Degree requirements in

**Mechanical Engineering**

**Moustafa Ahmed Hassan El Sayed Bakr**

**From**

**College of Engineering and Technology**

**AASTMT**

**Date: 17/04/2024**

**Supervisor:**

**Name:** Ass. Prof. Rola Afify

**Position:** Associate Professor, Mechanical Engineering Department, College of Engineering and Technology, Alexandria

**Signature:**

**Examiners:**

**Name:** Prof. EL Sayed Sabier

**Position:** Professor, Mechanical Engineering Department, College of Engineering and Technology, Alexandria

**Signature:**

**Name:** Prof. Yehia Eldrainy

**Position:** Associate Professor, Mechanical Engineering Department, College of Engineering and Technology, Alexandria

**Signature:**

---

**Name:** Ass. Prof. Rola Afify

**Position:** Associate Professor, Mechanical Engineering Department, College of Engineering and Technology, Alexandria

**Signature:**



**Arab Academy for Science, Technology and Maritime Transport**  
**College of Engineering and Technology Mechanical Engineering Department**  
**Mechanical Engineering Department**

MEng. Case Study Final Report

**Numerical and Experimental Study of a Cessna 182 Prototype**

**Presented by: Mostafa Ahmed Hassan EL Sayed Bakr**

**Supervised by: Ass. Prof. Rola Afify**

# DECLARATION

I hereby certify that this report, which I now submitting for assessment on the pregame of study leading to the award of Master of Engineering in Remote controlled aircraft model, is all my own work and contains no Plagiarism. By submitting this report, I agree to the following terms:

*Any text, diagrams, or other material copied from other sources (including, but not limited to, books, journals, and the internet) have been clearly acknowledge and cited followed by the references; either in the text or in a footnote/endnote. The detailed of the used references that are listed at the end of the report are confirming to the referencing style dictated by the final year project template and are, to my knowledge, accurate, and complete.*

I have read the sections on referencing and plagiarism in the final year project template. I understand that plagiarism can lead to a reduced or fail grade, in serious cases, for the MEng Course.

Student Name: Mostafa Ahmed Bakr	
Signed: _____	
Date: 06 / 03 / 2024	

# ACNOWLEDGMENT

Firstly, I thank Allah for helping me to complete this project

I would like to thank my case study supervisor Ass. Prof. Rola Afify for her efforts and great support which helped me to improve our performance and knowledge, since the very beginning as she helped me to discover the world of aerodynamics and AC aircrafts and made me looking forward to explore further in this overwhelming science.

Also, all thanks and respect to all staff members who taught me during the master semesters towards our MEng. degree in mechanical engineering.

I also thank Mr. Mahmoud Saad for helping me in manufacturing and proceeding through experimental part.

Special thanks for my parents for their endless efforts and unconditional support in all phases of my life especially in my education which lead me to this far of education.

# ABSTRACT

Aircraft designs rely on aerodynamics to understand how air flows and the generated lift and drag forces. This study investigates the fluid aerodynamics of a 1/5 scale Cessna 182 aircraft prototype using both experimental and numerical methods. The main objective is to analyze the drag force acting on the prototype and validate the findings through a comparative approach. In the Experimental Analysis, a prototype of 1/5 Cessna 182 was 3D printed and tested in a wind tunnel. Drag force acting on the prototype was directly measured using load cell, Arduino and software. Then, drag force is measured. In the Numerical Simulation, 1/5 scale Cessna 182 was produced using SolidWorks. Mesh independency was checked. Moreover, the model was meshed and analyzed using Ansys Fluent. Drag coefficient over the prototype was calculated. Furthermore, numerical study provided velocity distribution around the prototype, offering further insights into the airflow characteristics. For Comparison and Validation, the experimentally measured drag coefficient and the numerically calculated drag coefficient were compared. Good agreement was found between the two analyses. Using experimental and numerical analyses provide valuable data for understanding the aerodynamic performance of the Cessna 182 aircraft. The successful validation of the numerical simulation demonstrates its potential for further aerodynamic investigations and design optimization.

# TABLE OF CONTENTS

DECLARATION.....	V
ACNOWLEDGMENT.....	VI
ABSTRACT.....	V
TABLE OF CONTENTS.....	V
LIST OF Figures.....	V
Chapter One.....	1
INTRODUCTION.....	1
1.1 The Basic.....	1
1.2 WEIGHT .....	1
1.3 LIFT .....	2
1.4 DRAG.....	2
1.5 THRUST .....	2
1.6 PLANE COMPONENTS.....	2
1.7 WING .....	3
1.8 HORIZONTAL TAIL .....	3
1.9 VERTICAL TAIL.....	3
1.10 FUSELAGE.....	3
1.11 Characteristics and Features of RC Planes .....	3
1.12 RC-AIRCRAFT PROPULSION/POWER PLANTS.....	4
1.13 PROPELLER .....	4
1.14 MAIN GEAR OR LANDING GEAR.....	4
Chapter Two.....	6
Literature.....	6
Chapter Three.....	17
3.1 Steps.....	17
Chapter Four.....	24
4.1 introduction .....	25
4.2 SolidWorks drawings.....	25
4.3 Fluid Dynamics Contributions.....	25
4.3.1 Physical model .....	25
4.3.2 Numerical model .....	26
4.3.2.1. Domain dimensions.....	28
4.4 Results .....	29
4.4.1 Validation.....	29
Chapter Five.....	32
Results.....	33

## LIST OF Figures

<b>Fig. 3.1. Elevation view of Cessna 182.</b> .....	17
<b>Fig. 3.2. Cessna 182.</b> .....	17
<b>Fig. 3.3. Half the fuselage and a wing of Cessna 182.</b> .....	18
<b>Fig. 3.4. Three-dimensional printed fuselage part.</b> .....	18
<b>Fig. 3.5. Three-dimensional printed Wing parts.</b> .....	18
<b>Fig. 3.6. HAMPDEN H-6910-12-150-CDL Wind Tunnel220/380V - 50Hz.</b> .....	19
<b>Fig. 3.7. Plane prototype inside the wind tunnel.</b> .....	19
<b>Fig. 3.8. Fixed rod with the load cell.</b> .....	20
<b>Fig 3.9. Load Cell</b> .....	20
<b>Fig 3.10 Load Cell wiring.</b> .....	21
<b>Fig 3.11. Load Cell Connection.</b> .....	21
<b>Fig 3.12. Load Cell Interface with Arduino.</b> .....	22
<b>Fig 4.1. Prototype of 1/5 Cessna 182 SolidWorks model (a) Plan (b) Elevation</b> .....	25
<b>Fig 4.2 Half of Cessna 182 after SolidWorks drawing</b> .....	26
<b>Fig. 4.3. Cessna 182’s domain dimension Dim. in cm</b> .....	27
<b>Fig. 4.4. Cessna 182’s Boundary conditions.</b> .....	27
<b>Fig 4.5. Cessna 182’s outer domain.</b> .....	28
<b>Fig 4.6. Cessna 182’s inner domain. s</b> .....	28
<b>Fig 4.7. Cessna 182’s domain cross-section.</b> .....	29
<b>Fig. 4.8. Relation between Drag force and Air velocity for both numerical and experimental studies...</b>	30
<b>4 Fig. 4.9. Velocity distribution around the Cessna 182 prototype at air velocity of 35 m/s.</b> .....	30
<b>Fig. 4.10. Velocity distribution around the Cessna 182 prototype at air velocity of 35 m/s in a vertical plane.</b> .....	31
<b>Fig. 4.11. Streamlines around the Cessna 182 prototype at air velocity of 35 m/s in a vertical plane.</b> .....	31

## **INTRODUCTION**

The purpose of this project was to study the theory of flight, manufacture, and test a RC aircraft on a small domain to do this, knowledge of aerodynamics, structure mechanics, stability and weight balance needed to be applied.

For many people, drones and RC (remote-controlled) planes are both devices that fly in the air and are used for photography, racing, etc. However, there is much more to both drones and remote-controlled planes than this. That being said, what are the differences between the two?

Drones are small, unmanned aircraft built using sophisticated technology, unlike RC planes which are remotely piloted, small aircraft made from flimsy materials like foam. Both aircraft have a lot of differences in features and are used for different purposes.

For instance, RC planes cannot work without receiving signals from a radio transmitter and are primarily inefficient. In contrast, drones mostly fly independently and serve more purposes because of their efficiency.

### **1.1 THE BASICS**

The science of aerodynamics deals with the motion of air and the forces acting on bodies moving relative to the air **Roskam [1]**. Although aerodynamics is a complex subject, exploring the fundamental principles which govern flight can be an exciting and rewarding experience. The challenge to understand what makes an airplane fly begins with learning the four forces of flight.

### **1.2 WEIGHT**

Is the force produced by gravity pulling the plane towards the ground! All objects on Earth, including humans, are pulled towards the earth by gravity. The heavier the object is, the bigger this force is. If weight was the only force acting on the plane, it would fall straight down into the Earth. In order for the plane to fly, a second force must be acting on the plane to pull it upwards. We call this force lift.

### **1.3 LIFT**

Is produced by the plane as it travels through air, mostly by the plane's wings. A plane's wings have a special shape, called an airfoil, which forces air to flow over the top surface of the wing quicker than the bottom surface. The slow moving air beneath the wing puts more pressure on the bottom of the wing than the fast moving air on top, resulting in a force that pulls the plane up and balances the weight force.

### **1.4 DRAG**

Is also produced by the plane travelling through air. When objects move through fluids, like air and water, the fluid produces a force that opposes their motion. For instance, when you push a ball floating in water it will travel in the direction you push it, but it will slow down and eventually stop. This is because the water creates a force that pushes against the motion of the ball. Air acts the same way, so to keep a plane moving forwards at a constant speed, another force is needed to overcome drag.

### **1.5 THRUST**

Is the force produced by the plane's engines? This force pulls the plane forward through the air and overcomes the drag force produced by the air **Nelson [2]**. Planes can have a variety of engines to produce thrust, but the engines usually produce thrust by turning a propeller or accelerating a stream of air. Propellers have a number of blades that rotate and create forces to pull the plane through the air. Each blade has an airfoil cross-section, like a wing, and generates a lift force. Jet engines often have fans that act like propellers, but they also accelerate a narrow stream of air. The air moves much faster than the plane, but it has a lower mass. The momentum added to the stream of air is balanced by momentum added to the plane, which provides the thrust force.

### **1.6 PLANE COMPONENTS**

RC-aircraft are small model radio-controlled airplanes that fly using electric motors, gas powered IC engines or small model jet engines. The RC airplanes are flown remotely with the help of transmitter with joysticks that can be used to fly the aircraft and perform different maneuvers. The transmitter comes also with receivers which is installed inside the Model RC-aircraft which receives the commands send by the transmitter and controls servos. The servos are small motors which are mechanically linked to the control surfaces e.g., ailerons for roll control, elevator for pitch control and rudder for yaw control. The servos move the control rod (which are small rods that connect the servo to the different flight control e.g. to elevatored.)

which in turn moves the control surface be it elevator, flaps, aileron or rudder controlled in flight by using transmitter from where you control pitch, yaw and roll of your RC-aircraft and you also control the throttle settings. The receiver which accepts the transmitter signal and the servos attached to it are run on rechargeable.

## **1.7 WING**

**Etkin and Reid [3]** mention that wings are the main lifting body of the RC-aircraft providing the lift necessary for RC-aircraft flight. The wings provide lift because of aerodynamics shape which creates a pressure differential causing lift. If a cross-section of the wing is cut, a shape or profile is visible which is called an airfoil. Airfoil shape is the key to the wings ability to provide lift and is airfoil selection must be symmetric. On the wing flaps and ailerons.

## **1.8 HORIZONTAL TAIL**

The horizontal tail or the horizontal stabilizer provides pitch control to the RC airplane.

Elevator is mounted on the horizontal stabilizer or the horizontal tail of RC airplanes.

Normally, the horizontal tai is set at a -1-degree angle of attack (AOA) relative to the wing

## **1.9 VERTICAL TAIL**

The vertical tail or the vertical stabilizer provides yaw control to the RC airplanes.

Rudder is mounted to the vertical tail or vertical stabilizer of the RC airplanes.

## **1.10 FUSELAGE**

Fuselage is the main structural element of the RC-aircraft. The wing, horizontal and vertical tail are connected to the fuselage. The engine is also mounted to the fuselage is made up of bulk-heads. The bulk-heads are structural members which give strength and ridgity to the fuselage, support load and weight of the RC-aircraft. The engine bulk-head is made relatively stronger as compared to other bulk-heads of RC-aircraft fuselage because it carries the load of the engine as well as encounters vibrations during engine operations so it must be strong to resist al the loads.

The nose gear and main landing gear are also connected to the fuselage. The fuselage also houses all the electronic components necessary for RC-aircraft flight including ESC (electronic speed controller) in case of electric RC-aircraft, receiver, servos, batteries and fuel tank in case of gas-powered RC aircraft. External or internal payloads are also carried inside the fuselage.

The fuselage can be used to connected an external camera for example or to carry some payload inside the RC-aircraft.

### **1.11 Characteristics and Features of RC Planes**

RC planes are radio-controlled aircraft built from less sophisticated materials. **Jackson [5]** You can even easily make one in the comfort of your home. They are best for people just learning how to fly. RC planes are easily identified by their airplane-like shape, and do not have four rotors like most drones.

**Hoak [6]** The essential parts of an RC plane include nuts and bolts, electronic speed controller, electric propeller, battery, battery charger, foam board, radio transmitters, and receiver, control horns, etc. However, RC planes tend to be flimsy in structure and design. As such, they are also generally unstable in the air.

RC planes are used almost exclusively for entertainment purposes. You will rarely find someone who uses it for practical and commercial purposes such as videography, photography, etc. However, **Shevell [7]** some RC planes are more advanced in reporting navigational data.

### **1.12 RC-AIRCRAFT PROPULSION/POWER PLANTS**

RC-aircraft fly using either electric motor as propulsion device or IC (internal combustion) gas powered engines or small model jet Engines **Abbott [8]**.

### **1.13 PROPELLER**

The propeller is basically a wing section made of airfoil sections just like a wing but it is twisted along the span. The propeller is mounted to the engine in propeller driven RC-aircraft. Jet engine RC-aircraft don't have a propeller and generates thrust by means of the jet engine.

### **1.14 MAIN GEAR OR LANDING GEAR**

The main gear or landing gear is the main landing wheels of the RC-aircraft which takes the entire RC-aircraft. Main gear has to be strong and yet flexible enough to provide safe takeoff and landing to the RC-aircraft. **Lan [9]** A rigid flexible landing gear can damage the RC-aircraft structure as the entire weight/reaction force would be carried by the fuselage. So, in order to avoid this landing gears are designed to be strong yet flexible enough so they bend slightly during landing or takeoff to disperse the load and provides safe and smooth landing. Landing

gear or main gear consist of a pair of wheels which are generally larger in diameter as compared to the nose gear wheel. **Lan and Roskam [10]** The landing gear wheels are not steerable.

## *Chapter Two*

### *Literature*

**Welstead [11]** focused on incorporating stability and control into a multidisciplinary design optimization on a Boeing 737-class advanced concept called the D8.2b. He presented a new method of evaluating the aircraft handling performance using quantitative evaluation of the system to disturbances, including perturbations, continuous turbulence, and discrete gusts. He performed a multidisciplinary design optimization using the D8.2b transport aircraft concept. Moreover, he optimized the configuration for minimum fuel burn using a design range of 3,000 nautical miles and run cases using fixed tail volume coefficients, static trim constraints, and static trim and dynamic response constraints. However, he also used A Cessna 182T model to test the various dynamic analysis components to ensure that the analysis was behaving as expected. He found that stability and control should be included in conceptual design to avoid system level penalties later in the design process.

As unmanned air vehicles (UAVs) continue to expand their flight envelopes into areas of high angular rate and high angle of attack, modeling the complex unsteady aerodynamics for simulation in these regimes has become more difficult using traditional methods. **Hoe et al. [12]** experimentally aimed at improving the current six degree-of-freedom aerodynamic model of a small UAV by replacing the analytically derived damping derivatives with experimentally derived values. The UAV is named the Free-flying Aircraft for Sub-scale Experimental Research, FASER, and was tested in the NASA Langley Research Center 12-Foot Low-Speed Tunnel. The forced oscillation wind tunnel test technique was used to measure damping in the roll and yaw axes. By imparting a variety of sinusoidal motions, the effects of non-dimensional angular rate and reduced frequency were examined over a large range of angle of attack and side-slip combinations. Tests were performed at angles of attack from -5 to 40 degrees, sideslip angles of -30 to 30 degrees, oscillation amplitudes from 5 to 30 degrees, and reduced frequencies from 0.010 to 0.133. Additionally, the effect of aileron or elevator deflection on the damping coefficients was examined. Comparisons are made of two different data reduction methods used to obtain the damping derivatives. The results show that the damping derivatives are mainly a function of angle of attack and have dependence on the non-dimensional rate and reduced frequency only in the stall/post-stall regime.

A manned real-time simulation of a conceptual vehicle, the stratoplane, was developed to study problems associated with the flight characteristics of a large, lightweight vehicle. **Sim [13]** developed mathematical models of the aerodynamics, mass properties, and propulsion system

in support of the simulation and are presented. The simulation was at first conducted without control unaugmentation to determine the needs for a control system. The unaugmentation flying qualities were dominated by lightly damped dutch roll oscillations. Constant pilot workloads were needed at high altitudes. Control augmentation was investigated using basic feedbacks. For the longitudinal axis, flightpath angle and pitch rate feedback were sufficient to damp the phugoid mode and to provide good flying qualities. In the lateral-directional axis, bank angle, roll rate, and yaw rate feedbacks were sufficient to provide a safe vehicle with acceptable handling qualities. Intentionally stalling the stratoplane to very high angles of attack (deep stall) was investigated as a means to enable safe and rapid descent. It was concluded that the deep-stall maneuver is viable for this class of vehicle.

**Selig et al. [14]** design a new group of high-performance airfoils for radio controlled model sailplanes. As can be imagined, this involved numerous preliminary steps from preparing and instrumenting the tunnel to arranging for the models to be built, establishing a design procedure and, of course, solving all the myriad problems that occur in a multi-year project of this SIZE. In order to establish baseline data, a number of existing airfoil designs were tested first. These were selected primarily by the modeling community and are representative of what is presently used. They ranged from very simple, flat-bottom types, as well as some of the older NACA sections and their close derivatives, to very modern FAI-contest airfoils. Aside from providing the baseline, testing these airfoils allowed us to compare our data with other facilities where the same sections had also been tested. The flow behavior over an airfoil at high Reynolds numbers-greater, say, than 1-3 million-is well known. The boundary layer is laminar from the leading edge to a point typically near mid-chord where it makes a transition to turbulent flow. This transition, as well as the flow behind it, is generally well behaved. Unlike full-size airplanes, model sailplanes typically operate at chord Reynolds numbers between 50,000 and 500,000, often called the low Reynolds number regime. At these low Reynolds numbers, the flow is fundamentally different and more complicated than at high Reynolds numbers. The transition process is neither abrupt nor does it usually take place while the boundary layer is attached to the airfoil. Instead the laminar boundary layer separates, that is, it physically detaches from the airfoil surface. The flow then becomes unstable while separated, and makes the transition to turbulent flow in "mid-air." Only then does the flow reattach to the airfoil. And sometimes, if the laminar separation point is sufficiently far aft or if the Reynolds number is very low, the flow entirely fails to return to the airfoil surface. In either case large energy losses are associated with this process. This laminar separation, transition to turbulence, and turbulent reattachment enclose a region of recirculating flow aptly called the "laminar separation bubble." It is this extended transition process that is the principal reason for the degradation in

performance at low Reynolds numbers. Efforts towards drag reduction, therefore, largely concentrate on reducing the size and extent of the bubble.

**Schiestel and Chaouat [15]** gave a short retrospective review of the predictive methods of turbulent flows in Computational Fluid Dynamics over the last 50 years since the first development of computers. The divergent schools of turbulence modeling are presented with the aim to guide both users and researchers involved in numerical simulation of turbulent flows, Most of the turbulence numerical predictions are based on fully or partially-averaged statistical equations. Due to the turbulence closure problem, the equations to be solved more or less require modeling. Although one can conceptually distinguish the physical modeling corresponding to the constitutive laws of the turbulence from the numerical modeling corresponding to the algorithmic technique of the computational problem to solve, the two concepts are closely linked and progress together. The development of powerful computers allows solving more complex models. This retrospective landscape tries to point out the capabilities of the divergent models and the main cornerstones of their evolution in CFD research in relation to developments in computational capabilities. Evidently this review cannot be exhaustive at all, and references are given for the interested reader.

For hypersonic flight, the scramjet engine uses an isolator to contain the precombustion shock train formed by the pressure difference between the inlet and the combustion chamber. If this shock train were to reach the inlet, it would cause an engine unstart, disrupting the flow through the engine and leading to a loss of thrust and potential loss of the vehicle. Prior to this work, a Computational Fluid Dynamics (CFD) simulation of the isolator was needed for simulating and characterizing the isolator flow and for finding the relationship between back pressure and changes in the location of the leading edge of the shock train. **Hoeger [16]** employed a VULCAN code with back pressure as an input to obtain the time history of the shock train leading location. Results were obtained for both transient and steady-state conditions. His simulation showed a relationship between back-to-inlet pressure ratios and final locations of the shock train. For the 2-D runs, locations were within one isolator duct height of experimental results while for 3-D runs, the results were within two isolator duct heights.

**Soinneet [17]** investigated the application of CFD computations to flows around airplane ailerons combined with flight mechanical simulations to study the impact on airplane rolling maneuvers and aileron dynamics. The practical application is on Saab 2000 commuter airplane. In the validation of CFD computations the low speed airfoils FX 61-163 and FX 66- 17AII-182 were investigated with the 2D Navier-Stokes code ns2d by comparing the computations

with selected wind tunnel experiments. The medium speed MS(1)-0313 and the transonic DLBA032 airfoils with plain ailerons were investigated with ns2d and NSMB codes in selected wind tunnel cases representative for the ailerons of Saab 2000 aircraft. One algebraic and three k- $\epsilon$  turbulence models were used in the calculations at different aileron deflections. The effects of local mesh refinement and grid convergence were studied on the aerodynamic coefficients. Two-dimensional CFD computations were made on Saab 2000 aileron to compare the hinge moment with flight test results, measured by disconnecting the left and right hand side ailerons. The local angles of attack were determined by using extended lifting line theory and the conversion to 3D coefficients was made with handbook methods. The airplane rolling moment was determined by inserting the CFD derived lift effectiveness into the calculations. The effects of aileron slot and tab slot gap sizes as well as aileron hinge axis position on the aerodynamic coefficients were computed with the ns2d code. The CFD derived aerodynamic coefficients were fed into a six degree of freedom flight mechanical simulation system to study the impact on airplane rolling maneuvers. Frequency analysis was performed on the response of aileron deflection, airplane roll rate and roll acceleration to applied wheel force using fast Fourier transform, spectrum analysis and system identification. A review was made on practical aileron design considerations with issues on maximum wheel force, aileron effectiveness, wind tunnel testing, induced drag and aileron control system.

**Shawky et al [18]** presented modeling, guidance and control experimental results for a small unmanned aerial vehicle (UAV). The numerical values of the aerodynamic derivatives are computed via the Digital DATCOM software using the geometric parameters of the airplane. A hardware-in-the-loop (HIL) simulation environment is developed to support and validate the small UAV model autopilot hardware and software development. The HIL simulation incorporates a high-fidelity dynamic model that includes the sensor and actuator models, the test bed HIL system used to facilitate the development of the flight control system (FCS). Furthermore, design of the guidance laws, autopilot implementation on the embedded system are integrated with the HIL simulation. A mission has been design in order to validate the guidance and control loops. Finally, a user friendly graphical interface that incorporates external stick commands and 3-D visualization of the vehicle's motion completes the simulation environment.

**Ghika and Guerrero [19]** covered the phases from design to manufacturing of a wind tunnel test support structure for a conceptual blended wing body UAV designed by KTH Green Raven Project students. The innovative aircraft design demonstrates sustainability within aviation by utilizing a hybrid electric fuel cell propulsion system. The wind tunnel test to be conducted at

Bristol University will produce data to evaluate the aerodynamic properties of the model for design verification. The wind tunnel model is a small scaled 1.5m span model supported by struts that change the pitch and yaw angles during testing. An external force balance provided by Bristol University measures the loads and moments experienced by the model. The main requirements for the structure are to withstand the aerodynamic loads imposed by the model and to change the model's orientation while maintaining wind speed during the test. The maximum aerodynamic loads were provided in a matrix, the largest of which was used as the load condition for the support equating to a 512N lift at 14° AOA. Trade studies were conducted to determine the mechanisms to satisfy the requirements while staying within budget. The chosen design for the support structure includes a circular base plate constrained by a locking ring with positioning pins to change the yaw angle. The main strut is mounted at the center of the circular base plate. A hinge bracket at the top of the strut interfaces with another hinge bracket within the model via a clevis pin. An electric linear actuator mounted downstream of the main strut is used to vary the pitch angle, with the center of rotation at the clevis pin. Once the design was finalized, finite element analysis was done to verify the structural stability of the design. The FEA results were compared to Euler Bernoulli approximations for deflection. Manufacturing of the components was outsourced while assembly and programming of the actuator was done in-house.

The correlation of flight and wind-tunnel data has been the subject of considerable discussion for several decades. The success of these efforts has varied from complete failure to successful depending upon the class and complexity of configuration and performance level for which it was designed. **Saltzman and Ayers [20]** made a review to correlate flight and wind tunnel. They found that the discrepancies primarily involve Reynolds number and wall interference effects.

On the basis of the encouraging results of small-scale tests, **Weiberg and Gamse [21]** investigated the rotating cylinder flap principle applied to a large three-dimensional model. These tests were made to determine the rotating cylinder flap effectiveness and power requirements as affected by freestream velocity, propeller slipstream, cylinder peripheral speed, and ground proximity. The investigation included the effects of flap hinge line location on flap effectiveness, wing pitching moments, and flap hinge moments, and the effectiveness of slats and spoilers in conjunction with the rotating cylinder flap.

Experimental techniques to measure rotorcraft aerodynamic performance are widely used. However, most of them are either unable to capture interference effects from bodies, or require

an extremely large computational budget. **Koning [22]** developed an XV-15 Tilt Rotor Research Aircraft rotor model for investigation of wind tunnel wall interference using a novel Computational Fluid Dynamics (CFD) solver for rotorcraft, Rot-CFD. In Rot-CFD, a mid-fidelity URANS solver is used with an incompressible flow model and a realizable  $k-\epsilon$  turbulence model. The rotor is, however, not modeled using a computationally expensive, unsteady viscous body-fitted grid, but is instead modeled using a blade element model with a momentum source approach. Various flight modes of the XV-15 isolated rotor, including hover, tilt and airplane mode, have been simulated and correlated to existing experimental and theoretical data. The rotor model is subsequently used for wind tunnel wall interference simulations in the National Full-Scale Aerodynamics Complex (NFAC) at NASA Ames Research Center in California. The results from the validation of the isolated rotor performance showed good correlation with experimental and theoretical data. Their results were on par with known theoretical analyses. In Rot CFD the setup, grid generation and running of cases is faster than many CFD codes, which makes it a useful engineering tool. Performance predictions need not be as accurate as high-fidelity CFD codes, as long as wall effects can be properly simulated. For both test sections of the NFAC wall interference was examined by simulating the XV-15 rotor in the test section of the wind tunnel and with an identical grid but extended boundaries in free field. Both cases were also examined with an isolated rotor or with the rotor mounted on the modeled geometry of the Tiltrotor Test Rig (TTR). A ‘quasi linear trim’ was used to trim the thrust for the rotor to compare the power as a unique variable. Power differences between free field and wind tunnel cases were found from -7 % to 0 % in the 80- by 120-Foot Wind Tunnel test section and -1.6 % to 4.8 % in the 40- by 80-Foot Wind Tunnel, depending on the TTR orientation, tunnel velocity and blade setting. The TTR will be used in 2016 to test the Bell 609 rotor in a similar fashion to the research in this report

**Pettersson [23]** dealt with the problems of scaling aerodynamic data from the wind tunnel conditions to free flight. The main challenges when this scaling should be performed is how the model support, wall interference and the potentially lower Reynolds number in the wind tunnel should be corrected. Computational Fluid Dynamics (CFD) simulations have been performed on a modern transonic transport aircraft in order to reveal Reynolds number effects and how these should be scaled accurately. This investigation also examined how the European Transonic Wind tunnel (ETW) twin sting model support influences the flow over the aircraft. In order to further examine Reynolds number effects a MATLAB based code capable of extracting local boundary layer properties from structured and unstructured CFD calculations have been developed and validated against wind tunnel measurements. A general scaling methodology is presented.

**Greer et al. [24]** conducted a force-test investigation in the Langley full-scale wind tunnel to determine the static longitudinal and lateral stability and control characteristics of a full-scale mockup of a light single-engine high-wing airplane. Hinge moments were measured on all control surfaces during the investigation and downwash surveys were made at the horizontal tail. The investigation was made over an angle-of-attack range of  $-4^\circ$  to  $24^\circ$  at various angles of sideslip between,  $0^\circ$  for various power and flap settings. The power conditions were a thrust coefficient  $C_T$  of zero which represents either a low-power or a high-speed condition (where the thrust coefficient approaches zero),  $TI = 0.14$  which corresponds to a climb condition, and  $TI = 0.30$  which corresponds to a take-off condition. The investigation showed that the model has both stick-fixed and stick-free longitudinal stability up to the stall for all configurations tested with the center of gravity located at 13.7 percent of the mean geometric chord. Power generally has a small destabilizing effect, but at worst the model could become no more than neutrally stable with the center of gravity as far aft as 40 percent of the mean geometric chord. The model has positive effective dihedral and directional stability for all test conditions. The aileron and rudder effectiveness was maintained up to the stall and was powerful enough to trim out all model moments up to the stall.

While the “Numerical Wind Tunnel”, also known as a "digital wind tunnel", is closely associated with supercomputers, the system in a broader sense of its practicality, concepts, purposes, and achievements. **Matsuo [25]** addressed these questions, drawing on the numerical wind tunnel project pursued at the JAXA Chofu Aerospace Center, focusing on its historical context, current status, and future prospects, especially in connection with high-performance computing (HPC). The roots of numerical wind tunnel. To understand the numerical wind tunnel, we need first to give some background accounts regarding a "wind tunnel." JAXA describes a wind tunnel as an experimental facility used "to investigate aerodynamic characteristics (aerodynamics) and flow phenomena of the air surrounding aircraft or spacecraft. Airflow around aircraft can be simulated in a wind tunnel, which generates actual airflow artificially around an airframe model installed within the wind tunnel. By measuring some properties such as aerodynamic forces and pressure distributions around the model air frame, the wind tunnel allows us to grasp air behavior accurately." The model mentioned here is not at all like those fragile replicas one would imagine to see in a display cabinet. It must be a stiff model carved out of a metal block and so on, because it must endure tremendous force in high-speed wind tunnel testing. Fabricating the model is a costly and time-consuming process as it also requires high-precision work (Figure 1). Using a large-scale facility for testing requires dedicated specialist operators, and the test gives rise to a high energy cost. Therefore,

the tests involving a wind tunnel (wind tunnel testing) are generally expensive. Moreover, test conditions must be carefully considered and adjusted in order to obtain data on aerodynamic force and other parameters. However, once the test is ready to be executed, it proves to be remarkably efficient in terms of data productivity. For instance, it is possible to obtain approximately 200 cases of data per day where one case represents a combination of Mach number and elevation angle. These are the characteristics of wind.

With the continuous development and application of modeling technology, civil aircraft designers urgently need to apply model-based systems engineering (MBSE) theory and methods into the field of civil aircraft development. However, the existing modeling tools, which combined with MBSE methodologies, only focus on one particular area, such as requirement modeling, functional modeling and design synthesis. This kind of low coupling design system makes it difficult to link the upstream and downstream designers in the early stage of system development. **Bi et al. [26]** introduced the MBSE development process of civil aircraft and then establishes an integrated platform composed of six work stations for civil aircraft development based on this process. Commercially available modeling tools, such as IBM Rational DOORS and enterprise architect (EA), are conducted in the platform. The development of flight control system is taken as an example to test the feasibility and efficiency of our integrated platform in logic layer. This platform can complete the activities of aircraft life cycle function analysis, requirement and model management. The loose coupling between the modules and the high cohesive nature allows different system engineers to maintain their design independence and consistency at different stages of development.

Flight simulators play an important role in pilot training around the world. They contribute to increasing the safety of air traffic, allow you to practice dangerous situations and non-standard procedures and thus prepare pilots for dangers during real flight. **Janovec et al. [27]** dealt with the design and arrangement of the instrument part of the simulator, while the design is based mainly on the flight manual of the aircraft Zlín. The result of our work is the design of the structure, instrumentation of the simulator and the subsequent construction of the simulator. The created frame of the simulator construction, as a fixed platform, is used to place the computer technology and accessories of the simulator. The simulator will serve students of the Department of Air Transport for training procedures during the flight on a given type of aircraft, getting acquainted with the aircraft equipment, or training in non-standard and emergency situations.

Nowadays, Computational Fluid Dynamic (CFD) analysis is one of the most affordable techniques to determine the aerodynamic characteristics of an aircraft. It allows a development of advanced flight controllers. However, the accuracy of this technique depends on the input parameters such as the solid model. **Aati and Nejim [28]** described a methodology to estimate aerodynamic derivatives of a Cessna 182 aircraft based on solid model established by using photogrammetry technique. 312 images have been taken using Canon D750 camera with a 24 mm lens. A dense point cloud of the aircraft was generated using MicMac photogrammetry software. Then, the aircraft 3D-geometry was extracted in order to create the CAD model. Afterwards, parameters such as lift and drag coefficients were estimated at different angles of attack using Ansys Fluent software. The simulation results show that the lift and drag increase up to stall angle, then the lift starts to decrease. These results match the theoretical ones.

**Ananda et al. [29]** discussed the motivation, requirements, and approach of the University of Illinois at Urbana-Champaign (UIUC) General Aviation Upset and Stall Testing Aircraft Research (GAUSTAR) project. The goal of the GA-USTAR project is to build and flight test a dynamically-scaled, Reynolds number corrected model of a General Aviation (GA) type aircraft intended for upset and stall flight modeling. The project is separated into three phases. In Phase 1, to simplify the construction, a scaled commercial-of-the-shelf radio control (R/C) model of a GA aircraft is used as a starting point. From a list of available GA aircraft R/C models, a 1-5-scale Cessna 182 was selected. The methodology behind the choice of the Cessna 182 as the GA-USTAR Phase 1 (baseline) model is detailed. The method of accurately determining the mass distribution and inertias is described in detail. In Phase 2, the approach taken to appropriately dynamically scale the Phase 1 Cessna 182 model is discussed. The desired geometric, kinematic, and mass parameters for a dynamically-scaled Cessna 182 is discussed. Finally, to ensure that stall is closely matched, new airfoils will be designed and tested in the UIUC subsonic wind tunnel and then used on the GA-USTAR Phase 3 flight platform. New airfoils are required to correct for the Reynolds number effects inherent in scaled models. Flight testing and data acquisition will be performed for all three phases of the GA-USTAR project. Details regarding flight data instrumentation and flight test planning are also described in this paper.

**For a 1-5th-scale R/C model of the Cessna 182, Vahora et al. [30]** discussed the aerodynamic scaling process of a 1-5th-scale R/C model of the Cessna 182 for the General Aviation Upset and Stall Testing Aircraft Research (GA-USTAR) project. The GA-USTAR project aims to construct a dynamically-scaled model of typical General Aviation aircraft for the purpose of validating flight simulator stall/upset models. Modeling the stall behavior of a scaled aircraft

requires aerodynamic scaling to account for changes in the operating Reynolds number. Aerodynamic scaling of the Cessna 182 was accomplished through the design of a new wing airfoil that matched the lift curve slope, maximum lift coefficient, and the moment coefficient of the wing airfoil (NACA 2412) of the full-scale Cessna 182 at stall conditions. To accomplish this, an in-house developed inverse airfoil design tool, PROFOIL, was used to design the VAS1715 airfoil. The VAS1715 airfoil, is 12% thick and has a maximum camber of 5.16%. The VAS1715 airfoil was designed to have the same maximum lift coefficient at a Reynolds number of 230,000 (scaled Cessna 182 stall Re) as the NACA 2412 airfoil at a Reynolds number of 2,700,000 (full-scale Cessna 182 stall Re). Verification of the designed VAS1715 airfoil performance was carried out by performing experimental validation using the University of Illinois at Urbana-Champaign (UIUC) Low Speed Airfoil Testing setup at the UIUC Aerodynamic Research Lab for Reynolds numbers ranging from 200,000 to 450,000. For each of Reynolds numbers tested lift and moment of the VAS1715 airfoil were measured for angles of attacks from -10 to 20 deg to obtain the linear and post-stall range. The drag for each Reynolds number was measured separately using a wake rake from -10 to ~14 deg (up to stall). Measured experimental VAS1715 airfoil performance data are summarized in this paper together with discussion of the results and its matching with NACA 2412 airfoil (full-scale Cessna 182 wing airfoil) results.

General Aviation Upset and Stall Aircraft Recovery (GA-USTAR) is a project being conducted by the Applied Aerodynamics Group at the University of Illinois at Urbana-Champaign. GA-USTAR aims to construct a 1-5th dynamically-scaled Cessna 182 model to validate upset and stall flight simulations for general aviation aircraft. Dynamic scaling is the process by which a scale model of an aircraft can be modified to match the flight characteristics of the full-scale through scaling of mass and other properties. **Qadri et al. [31]** detailed the contributions of undergraduate research assistants in the development of the GA-USTAR project and the subsequent educational value of undergraduate research. The undergraduate contributions discussed in this paper include the building of a stock Top Flite Cessna 182 Skylane model for baseline testing, determination of modifications necessary to dynamically scale the model to match the mass properties of the full-scale, creation of a weighted CAD model of the scale model, as well as initial flight testing. Through participation, the undergraduate research assistants gained valuable skills, experience, and insight applicable in both academia and industry that they would not have otherwise obtained through the undergraduate curriculum.

**Vahora et al. [32]** discussed the aerodynamic scaling process of a 1-5th-scale R/C model of the Cessna 182 for the General Aviation Upset and Stall Testing Aircraft Research (GA-

USTAR) project. The GA-USTAR project aims to construct a dynamically-scaled model of typical General Aviation aircraft for the purpose of validating flight simulator stall/upset models. Modeling the stall behavior of a scaled aircraft requires aerodynamic scaling to account for changes in the operating Reynolds number. Aerodynamic scaling of the Cessna 182 was accomplished through the design of a new wing airfoil that matched the lift curve slope, maximum lift coefficient, and the moment coefficient of the wing airfoil (NACA 2412) of the full-scale Cessna 182 at stall conditions. To accomplish this, an in-house developed inverse airfoil design tool, PROFOIL, was used to design the VAS1715 airfoil. The VAS1715 airfoil, is 12% thick and has a maximum camber of 5.16%. The VAS1715 airfoil was designed to have the same maximum lift coefficient at a Reynolds number of 230,000 (scaled Cessna 182 stall Re) as the NACA 2412 airfoil at a Reynolds number of 2,700,000 (full-scale Cessna 182 stall Re). Verification of the designed VAS1715 airfoil performance was carried out by performing experimental validation using the University of Illinois at Urbana-Champaign (UIUC) Low Speed Airfoil Testing setup at the UIUC Aerodynamic Research Lab for Reynolds numbers ranging from 200,000 to 450,000. For each of Reynolds numbers tested lift and moment of the VAS1715 airfoil were measured for angles of attacks from -10 to 20 deg to obtain the linear and post-stall range. The drag for each Reynolds number was measured separately using a wake rake from -10 to ~14 deg (up to stall). Measured experimental VAS1715 airfoil performance data are summarized in this paper together with discussion of the results and its matching with NACA 2412 airfoil (full-scale Cessna 182 wing airfoil) results.

## Chapter Three

### Experimental Analysis

#### 3.1 Steps:

For the experimental analysis, a three-dimensional drawing was first made via SolidWorks, Figs. 3.1 to 3.3. Then, a three-dimensional printed model of the Cessna 182 was created in two symmetrical halves, Figs. 3.4 and 3.5. These two parts were combined and placed inside the wind tunnel, Fig. 3.6. Once the model was positioned, a load cell, Arduino and software were employed to measure the drag force acting on the aircraft.

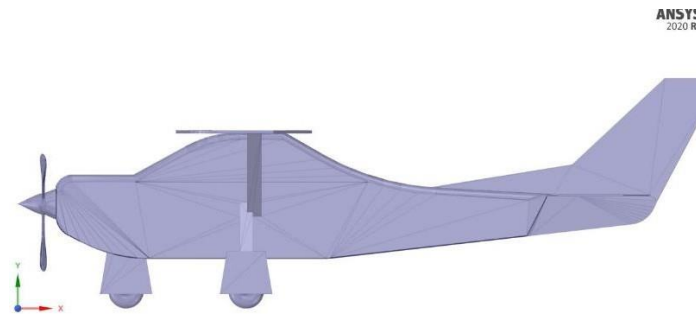


Fig. 3.1. Elevation view of Cessna 182.

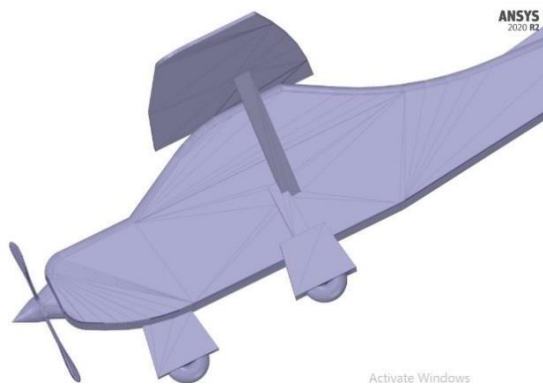


Fig. 3.2. Cessna 182.

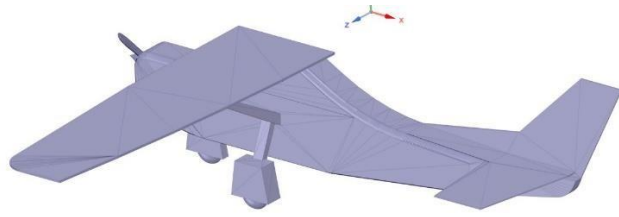


Fig. 3.3. Half the fuselage and a wing of Cessna 182.

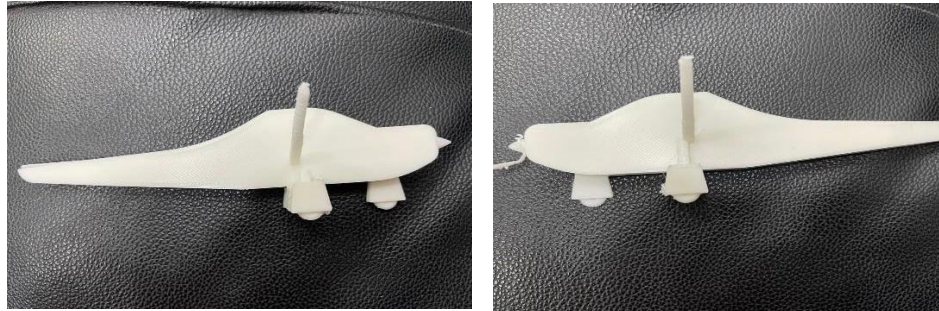


Fig. 3.4. Three-dimensional printed fuselage part.

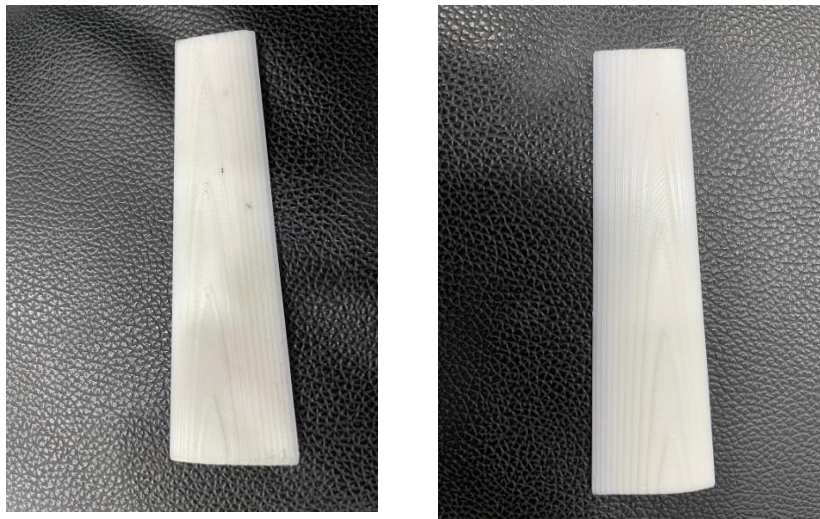


Fig. 3.5. Three-dimensional printed Wing parts.

Wind tunnels are tubular devices that simulate air flow over objects, allowing researchers to study their aerodynamics. Invented for aeronautics, they've become crucial for testing buildings, cars, and more, influencing design and safety.

The manometers utilized on the Hampden H-6910-12-150-CDL Wind Tunnel are well type with precision bored wells. The lift and drag option on the H-6910-12-150 allows measurement of lift and drag forces on various shapes placed in the wind tunnel's air stream. The readings are displayed on a digital meter and the selection between lift and drag is accomplished with the toggle switch located on the meter's front panel.

Wind tunnel parts are:

1. Contraction
2. Test section
3. Diffuser
4. Driver Motor
5. Compressor or Fan
6. Acoustic muffler
7. Vanes



Fig. 3.6. HAMPDEN H-6910-12-150-CDL Wind Tunnel 220/380V - 50Hz.

Two symmetric parts of plane prototype are combined together with a rod connected them to a load cell, Fig. 3.7. Put the plane into the wind tunnel, Fig. 3.8.

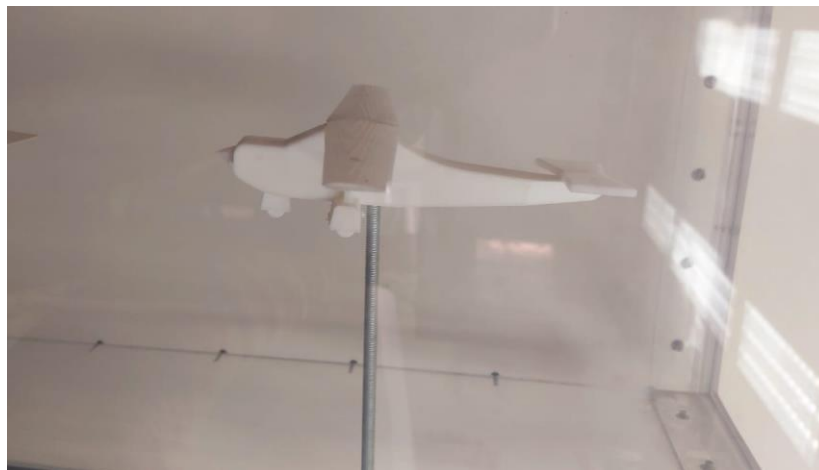


Fig. 3.7. Plane prototype inside the wind tunnel.

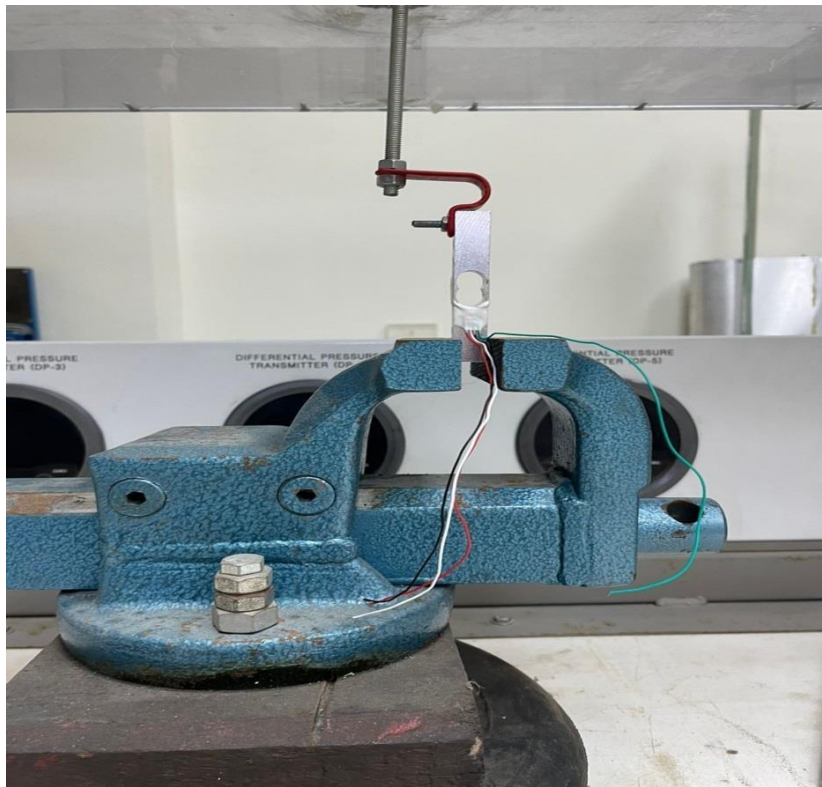


Fig. 3.8. Fixed rod with the load cell.

To measure the drag force, a beam type load cell is selected to be used, Fig. 3.9. Beam type load cells are commonly employed for measuring low-level loads. The load cell of capacity 10 N is used as a simple cantilever beam serves as the elastic member to measure the drag force acting on the blade of the turbine. Two strain gauges on the top surface and two strain gauges on the bottom surface (all oriented along the axis of the beam) act as the sensor. The gages are connected into a Wheatstone bridge for load cell wiring, Figs. 3.10 to 3.12.

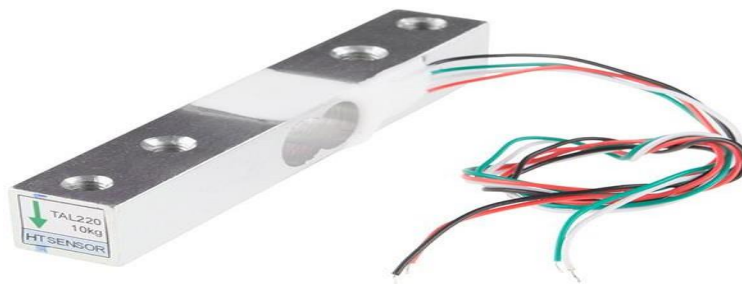


Fig 3.9. Load Cell.

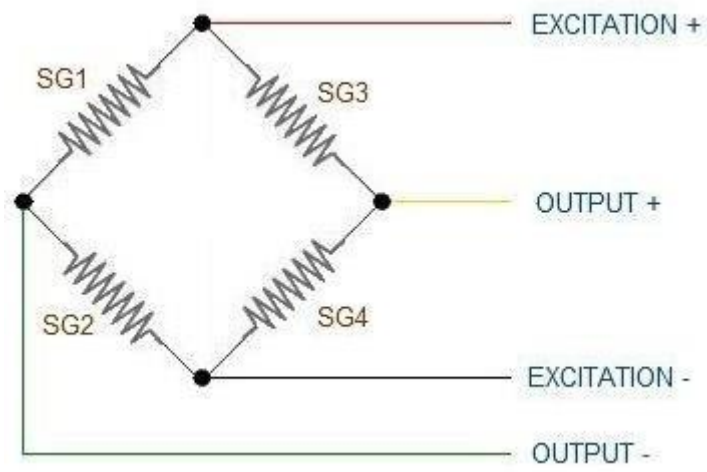


Fig 3.10 Load Cell wiring.

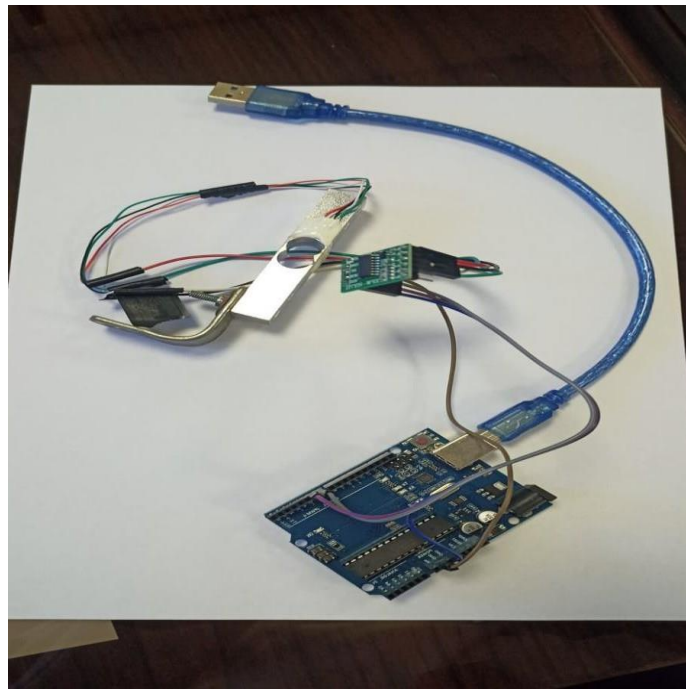


Fig 3.11. Load Cell Connection.

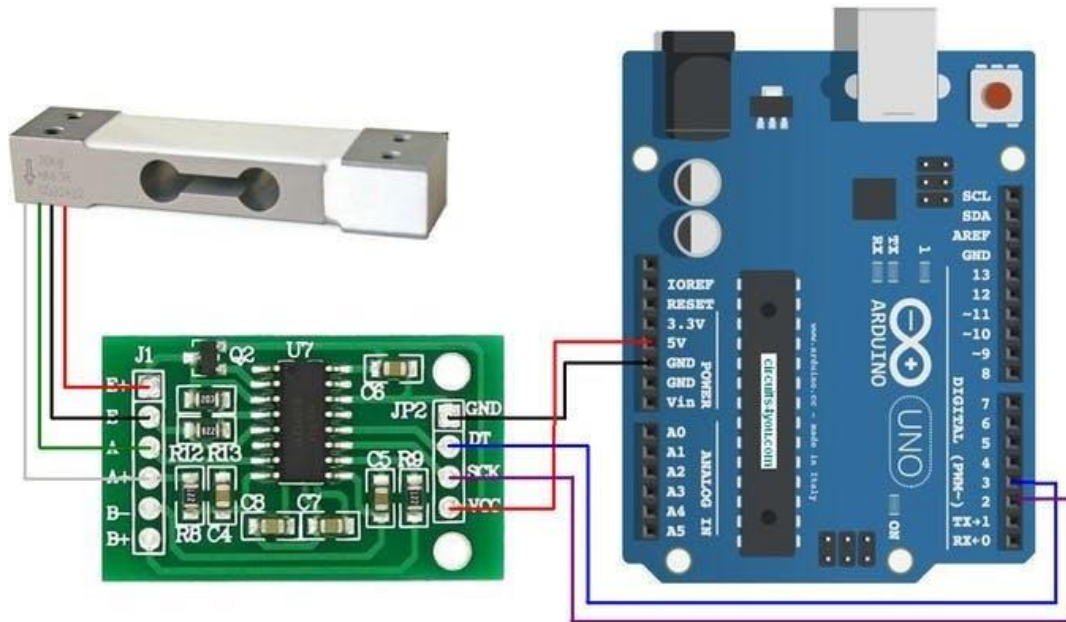


Fig 3.12. Load Cell Interface with Arduino.

Finally, drag force Measurement Code used in Arduino is as follows:

```
float L=170.0;
#include "HX711.h"
#define calibration_factor 109.5 //This value is obtained using the
SparkFun_HX711_Calibration sketch (103.55)
#define DOUT 3
#define CLK 2
HX711 scale(DOUT, CLK);
void setup() {
  Serial.begin(9600);
  Serial.println("HX711 scale");
  scale.set_scale(calibration_factor); //This value is obtained by using the
SparkFun_HX711_Calibration sketch
  scale.tare(); //Assuming there is no weight on the scale at start up, reset the scale to 0
  Serial.println("Readings:");
}
void loop() {
```

```

Serial.print("DF: ");

Serial.print(scale.get_units()*(9.81*170.0*0.059812)/(1000.0*L), 3); //scale.get_units()
returns a float

Serial.println(" N");

delay(200);

}

Torque cell code

#include "HX711.h"

#define calibration_factor 1000.0 //This value is obtained using the
SparkFun_HX711_Calibration sketch (100000.0)

#define DOUT 3

#define CLK 2

HX711 scale(DOUT, CLK);

void setup() {

  Serial.begin(9600);

  Serial.println("HX711 scale demo");

  scale.set_scale(calibration_factor); //This value is obtained by using the
SparkFun_HX711_Calibration sketch

  scale.tare(); //Assuming there is no weight on the scale at start up, reset the scale to 0

  Serial.println("Readings:");

}

void loop() {

  Serial.print("T: "); //You can change this to kg but you'll need to refactor the calibration_factor

  Serial.print((scale.get_units()*10.84+361.4)+8, 3); //scale.get_units() returns a float

  Serial.println(" N mm "); //You can change this to kg but you'll need to refactor the
calibration_factor

  delay(200);

```

# Design and 3D CFD Static Verification and Validation in Computational Fluid Dynamics

## **4.1 introduction**

During the last three or four decades, computer simulations of physical processes have been used in scientific research and in the analysis and design of engineered systems. The systems of interest have been existing or proposed systems that operate at design conditions, off-design conditions, failure-mode conditions, or accident scenarios. The systems of interest have also been natural systems. For example, computer simulations are used for environmental predictions, as in the analysis of surface-water quality and the risk assessment of underground nuclear-waste repositories. These kinds of predictions are beneficial in the development of public policy, in the preparation of safety procedures, and in the determination of legal liability. Thus, because of the impact that modeling and simulation predictions can have, the credibility of the computational results is of great concern to engineering designers and managers, public officials, and those who are affected by the decisions that are based on these predictions.

For engineered systems, terminology such as virtual prototyping and virtual testing is now being used in engineering development to describe numerical simulation for the design, evaluation, and testing of new hardware and even entire systems. This new trend of modeling and-simulation-based design is primarily driven by increased competition in many markets, e.g., aircraft, automobiles, propulsion systems, and consumer products, where the need to decrease the time and cost of bringing products to market is intense. This new trend is also driven by the high cost and time that are required for testing laboratory or field components, as well as complete systems. Furthermore, the safety aspects of the product or system represent an important, sometimes dominant element of testing or validating numerical simulations. The potential legal and liability costs of hardware failures can be staggering to a company, the environment, or the public. This consideration is especially critical, given that the reliability, robustness, or safety of some of these computationally based designs are high-consequence systems that cannot ever be tested. Examples are the catastrophic failure of a full-scale containment building for a nuclear power plant, a fire spreading through (or explosive damage to) a high-rise office building, and a nuclear weapon involved in a ground-transportation accident. In computational fluid dynamics (CFD) research simulations, in contrast, an inaccurate or misleading numerical simulation in a conference paper or a journal article has comparatively no impact

## **4.2 SolidWorks drawings**

To verify the same results between experimental and numerical, the same SolidWorks drawing of the prototype of 1/5 Cessna 182 was used, Fig. 4.1.

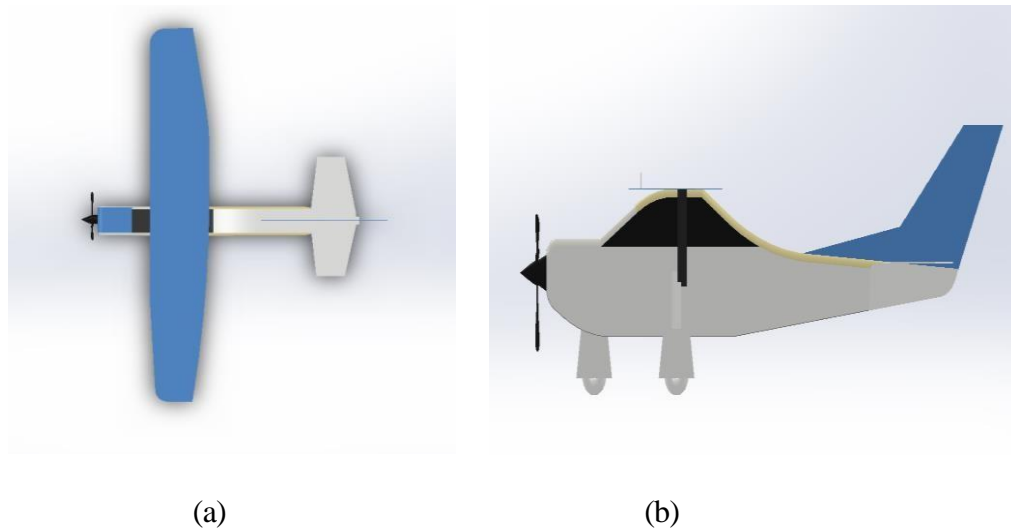


Fig 4.1. Prototype of 1/5 Cessna 182 SolidWorks model (a) Plan (b) Elevation.

## **4.3 Fluid Dynamics Contributions:**

CFD is one of the first fields to seriously begin developing concepts and procedures for V&V methodology. Literature has identified a number of authors who have contributed to the verification of CFD solutions. Most of these authors have contributed highly accurate numerical solutions, while some have contributed analytical solutions useful for verification. In addition, several of these authors have contributed to the numerical methods needed in verification activities, e.g., development of procedures using Richardson extrapolation. Note, however, that many of these authors, especially those in the early years, do not refer to verification or may even refer to their work as validation benchmarks. This practice simply reflects the past, and even present, confusion and ambiguity in the terminology. Several textbooks also contain a number of analytical solutions that are useful for verification of CFD codes. Work in validation methodology and validation experiments has also been conducted by a large number of researchers through the years.

In the present study, three-dimensional numerical simulations are used to calculate the static torque of the Cessna 182 and to show its air flow velocity and streamlines distributions.

### **4.3.1 Physical model**

Fig. 4.2 shows the steps used in SolidWorks to draw the Cessna 182. It consists of many parts and wing has its own airfoil and also the tail part. Trimming was used and dimensions were applied with a mirror step after the fuselage and the wing were sketched

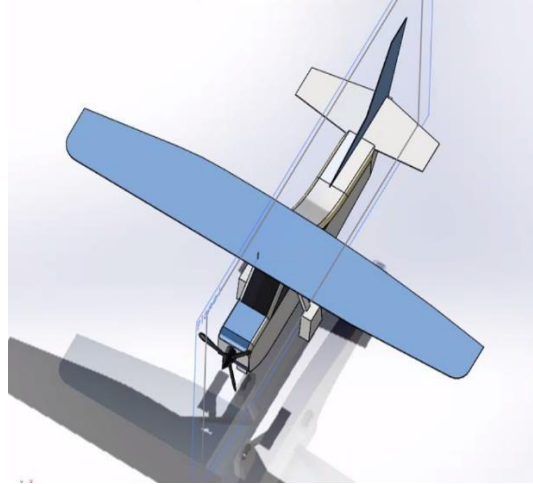
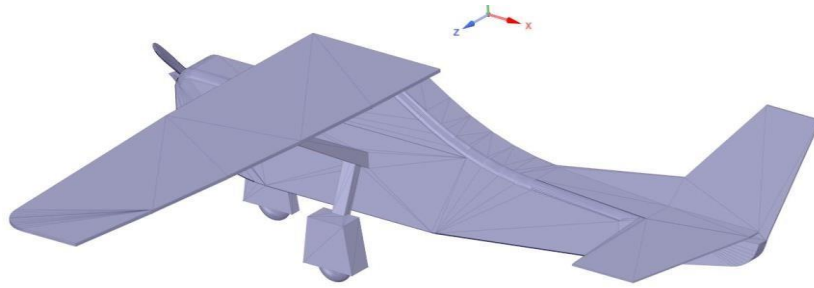


Fig 4.2 Half of Cessna 182 after SolidWorks drawing

## 4.3.2 Numerical model

Simulations of air flow around the plane were conducted using Ansys FLUENT after setting the test conditions to be similar to real conditions.

### 4.3.2.1. Domain dimensions

The numerical domain included the airplane and the air around the airplane. It contains two domains; inner and outer domain, Fig. 4.3. The inner domain is 80 cm width, 75 cm length and 30 cm height. The outer domain is 200 cm width, 250 cm length and 90 cm height.

Boundary conditions are walls for airplane, interface for all inner domain boundaries, inlet for the left vertical boundary, outlet for the right vertical boundary, and symmetry for other sides, top, and bottom boundaries, Fig. 4.4.

Meshes are shown in Figs. 4.5, 4.6, and 4.7 for outer domain, inner domain, and cross-section, respectively.

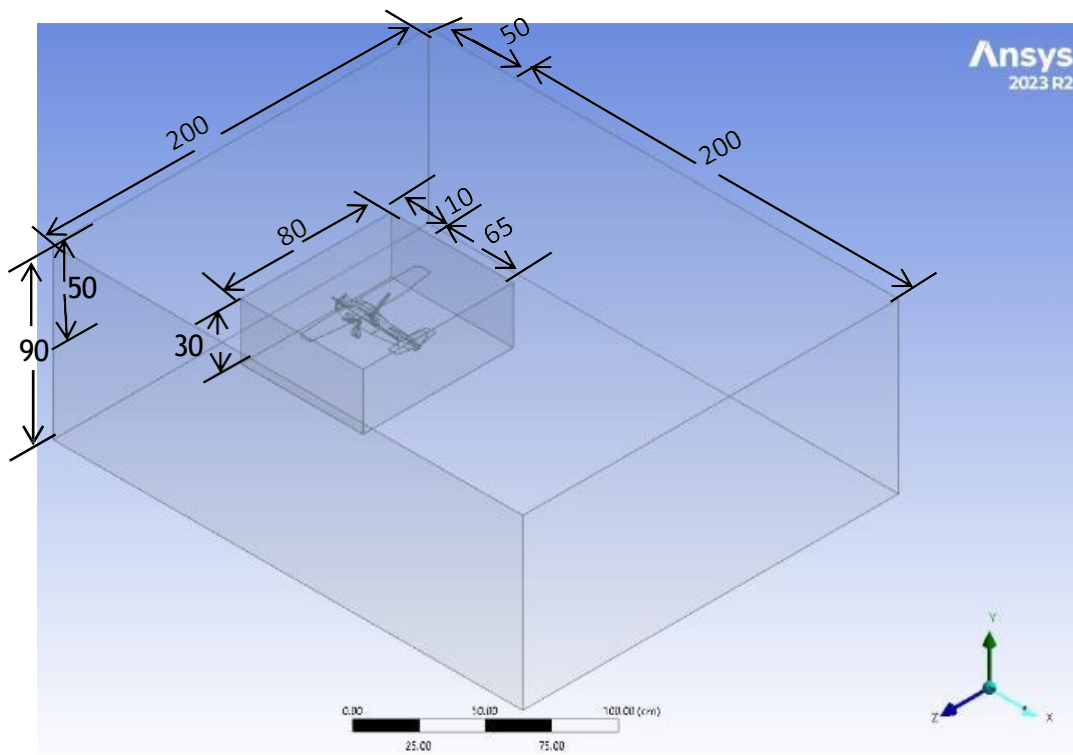


Fig. 4.3. Cessna 182's domain dimension Dim. in cm.

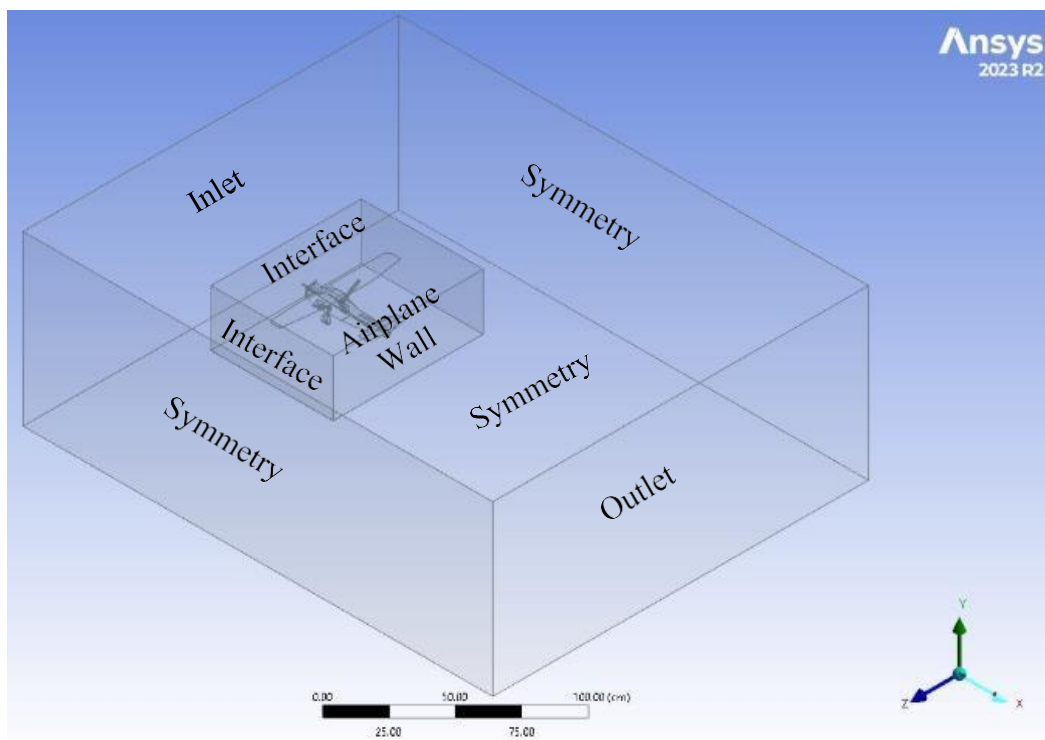


Fig. 4.4. Cessna 182's Boundary conditions.

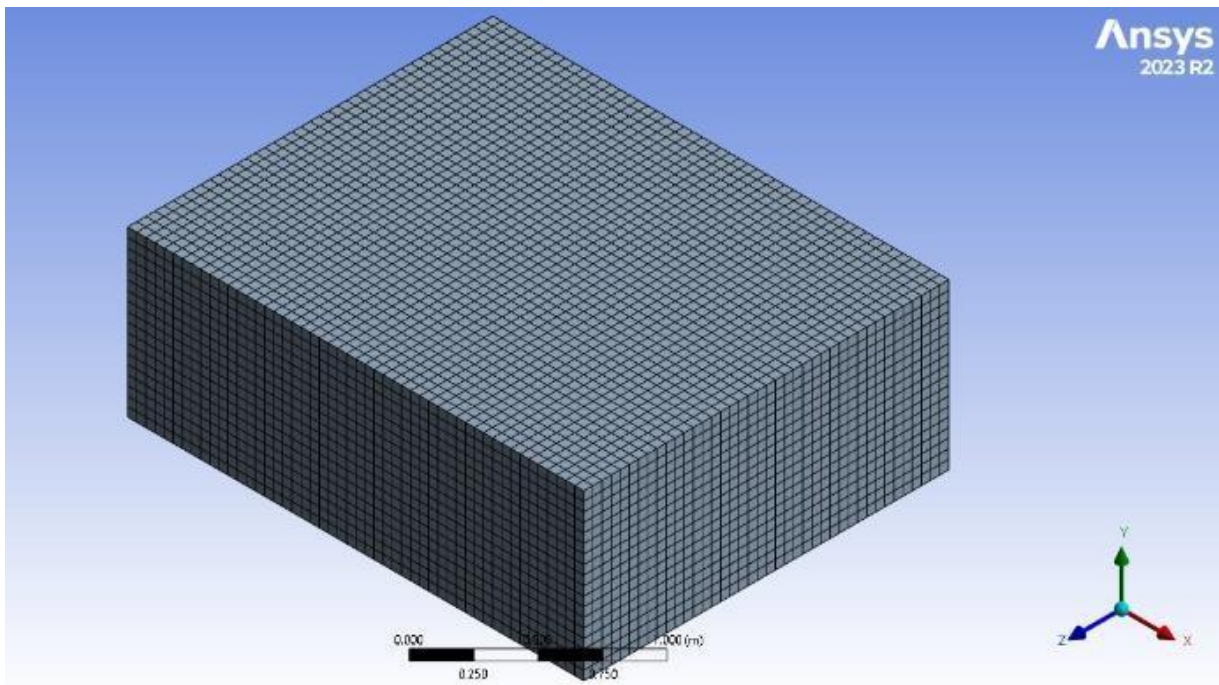


Fig 4.5. Cessna 182's outer domain.

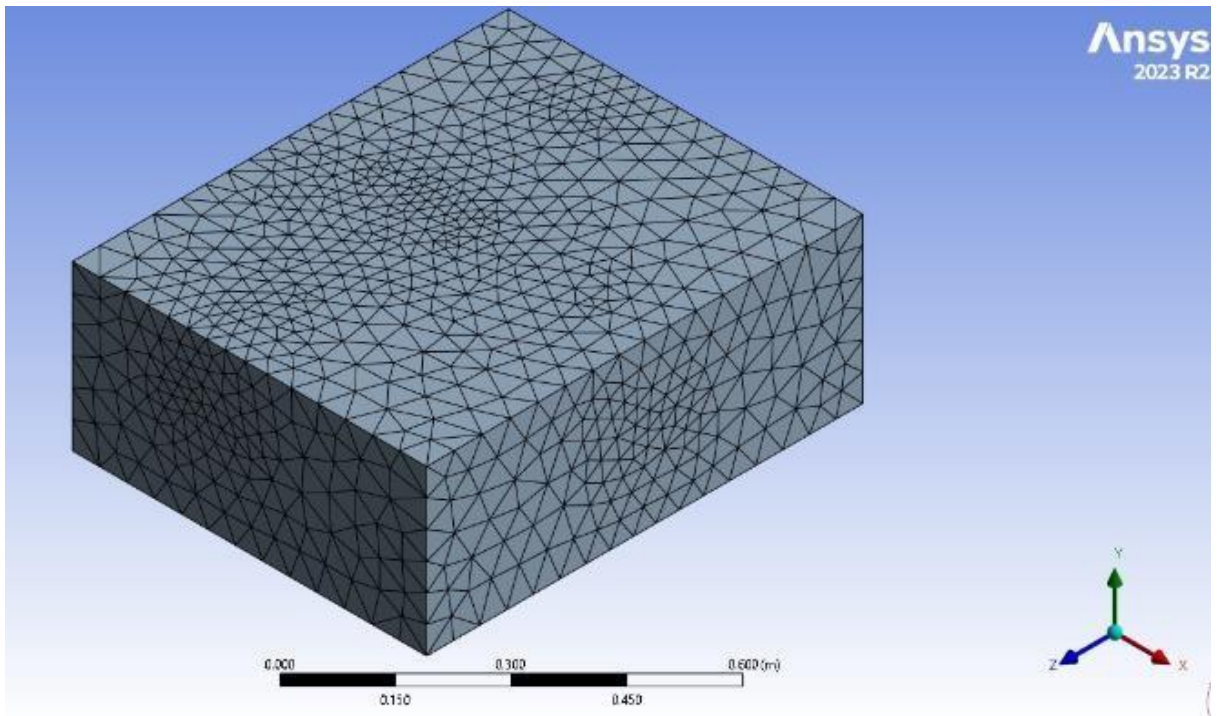


Fig 4.6. Cessna 182's inner domain.

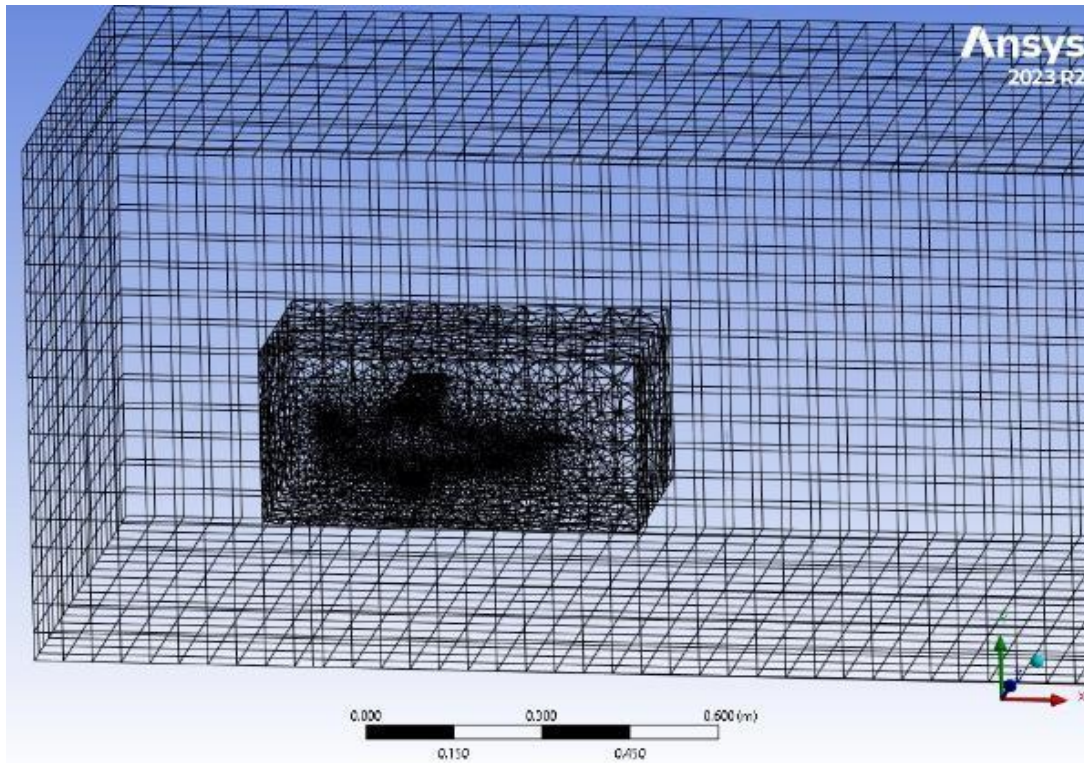


Fig 4.7. Cessna 182's domain cross-section.

K- $\omega$  SST Model was used. Airplane material was selected to be aluminum. The whole domain was Air. For boundary conditions, the left boundary was defined as a velocity inlet. The air flow has a wind velocity of 45 m/s. Residuals were used to be 0.0001. Hybrid initialization is selected. Time step size of  $2e-5$  was used.

## **4.4 Results**

### **4.4.1 Validation**

To confirm that numerical analysis has a correct coefficient of drag value, a validation between experimental and numerical analyses has been made. Fig. 4.8 shows the relation between Drag coefficient and air velocity for both numerical and experimental studies. It can be dedected a good agreement.

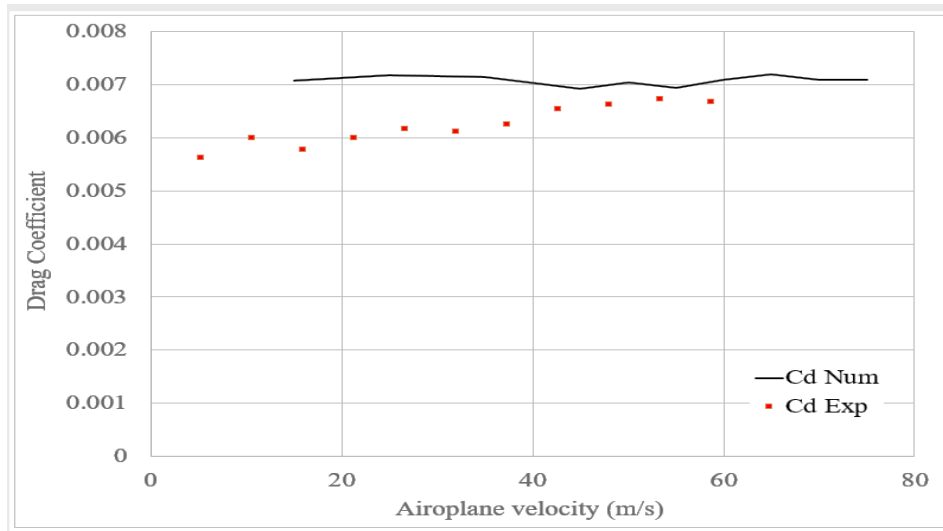


Fig. 4.8. Relation between Drag force and Air velocity for both numerical and experimental studies.

Figs. 4.9 and 4.10 show the velocity distribution around the Cessna 182 prototype at an air velocity of 35 m/s. Moreover, Fig. 4.11 shows streamlines at an air velocity of 35 m/s. It can be noticed that there are no eddies in the wake of the airplane. This means that a good design has been selected of Cessna 182.

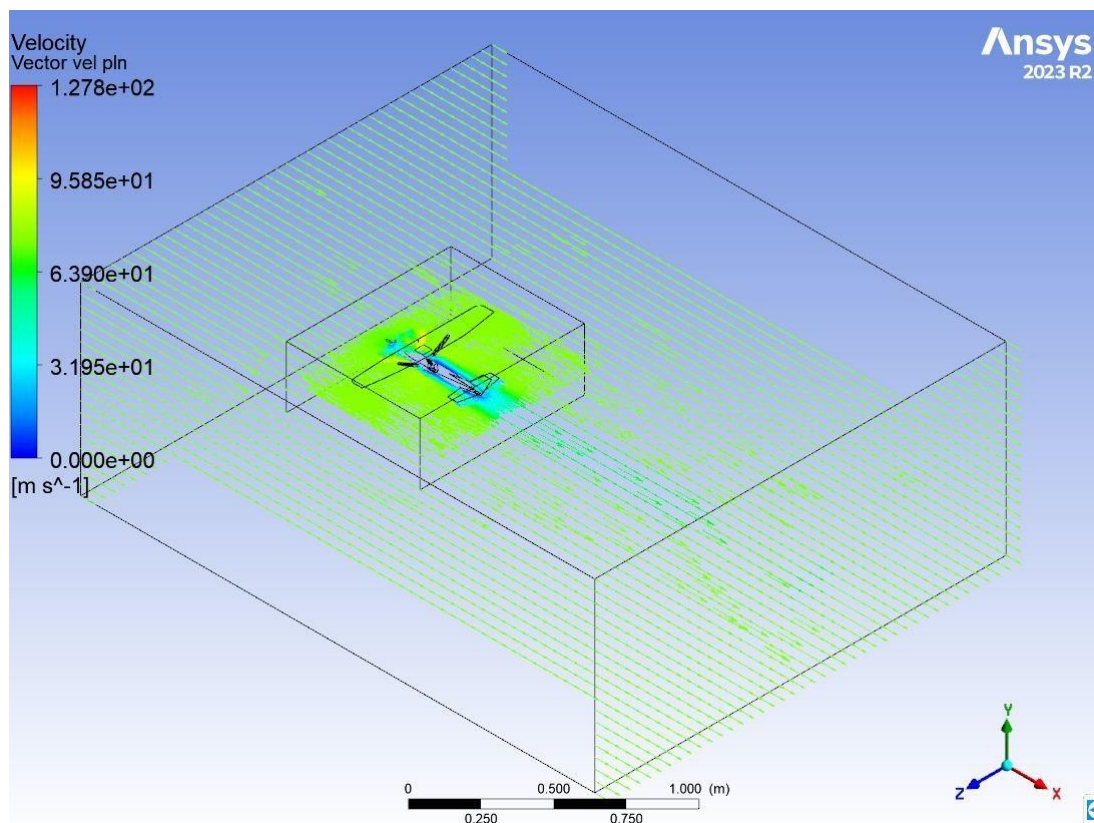


Fig. 4.9. Velocity distribution around the Cessna 182 prototype at air velocity of 35 m/s.

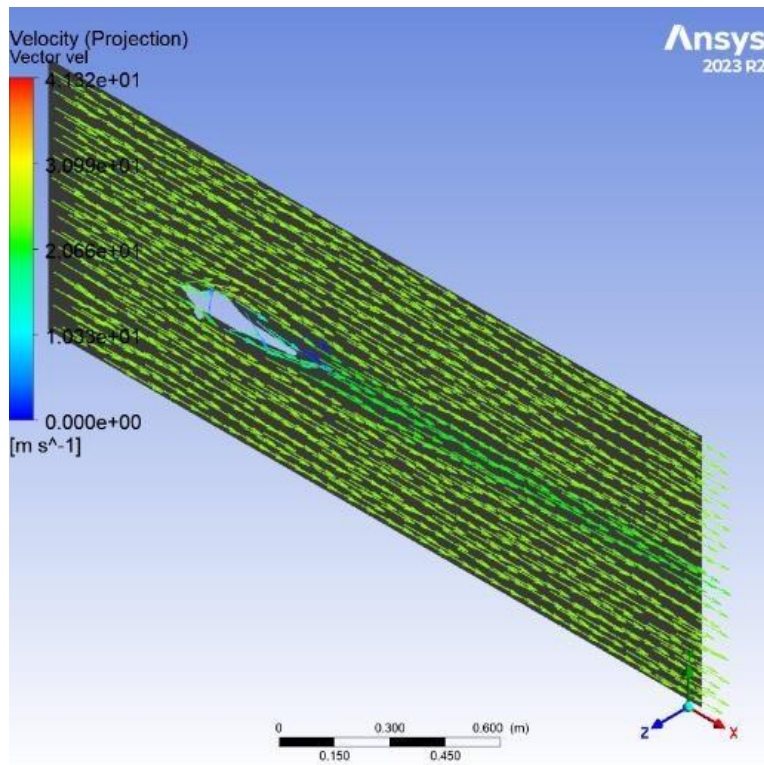


Fig. 4.10. Velocity distribution around the Cessna 182 prototype at air velocity of 35 m/s in a vertical plane.

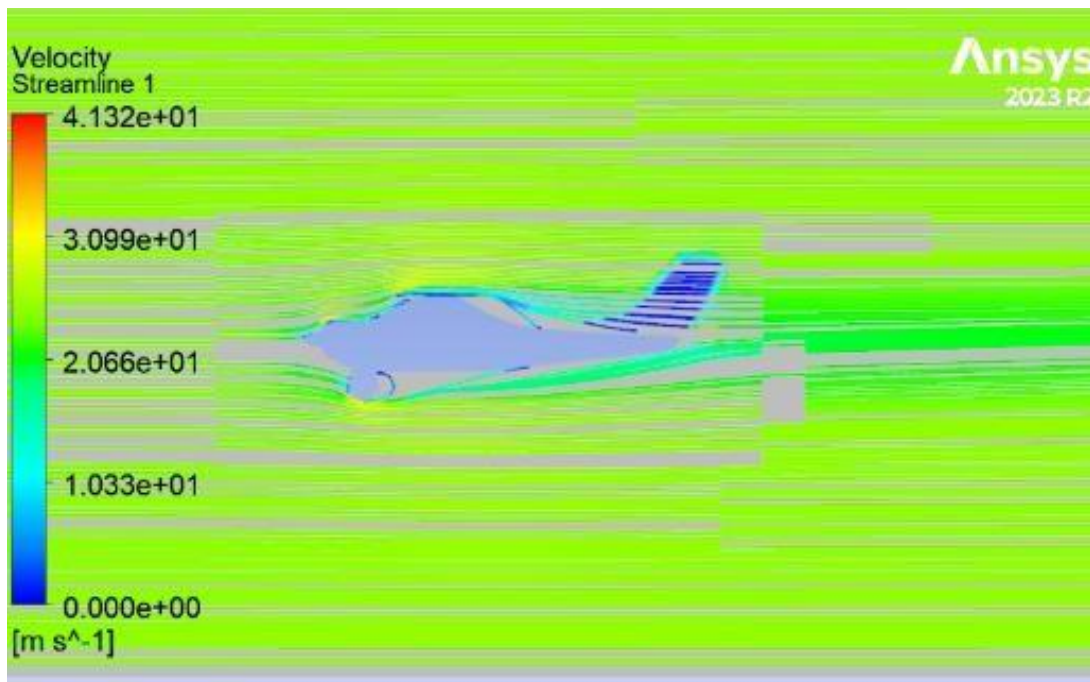


Fig. 4.11. Streamlines around the Cessna 182 prototype at air velocity of 35 m/s in a vertical plane.

## *Chapter Five*

### *Conclusion*

This study successfully investigated the drag characteristics of a 1/5 scale Cessna 182 prototype using both wind tunnel experimental analysis and Ansys Fluent numerical simulations. The obtained drag coefficient values showed good agreement between the two methods. Additionally, the numerical simulation provided valuable insights into the velocity distribution around the prototype. The achieved drag coefficient value of approximately 0.007 indicates a well-designed aircraft with minimal drag, contributing to its efficient performance. Further studies could explore the impact of different configurations and flight conditions on the Cessna 182's aerodynamics using the validated numerical model.

## References

1. Roskam, J. "Airplane Flight Dynamics and Automatic Flight Control Part I", DAR Corporation, 2007.
2. Nelson, R. "Flight Stability and Automatic Control", McGraw-Hill, 1997.
3. Etkin, B. and Reid, L.D. "Dynamics of Flight Stability and Control", 3rd edn, John Wiley & Sons, Inc. 1995.
4. "Federal Aviation Regulations, Federal Aviation Administration, Department of Transportation", 2011.
5. Jackson, P. Jane's "All the World's Aircraft", Jane's Information Group, various years., 1995.
6. Hoak, D.E., Ellison, D.E., Fink, R.D. et al. "USAF Stability and Control DATCOM, Flight Control Division, Air Force Flight Dynamics Laboratory", Wright-Patterson AFB, Ohio., 1978.
7. Shevell, R.S. "Fundamentals of Flight, 2nd edn", Prentice Hall., 1989.
8. Abbott, I.H. and Von Donehoff, A.F. "Theory of Wing Sections", Dover, 1959.
9. Lan, E.C.T., "Applied Airfoil and Wing Theory", Cheng Chung Book Company., 1988
10. Lan, E.C.T. and Roskam, J., "Airplane Aerodynamics and Performance", DAR Corporation, 2003.
11. Welstead, J., "Conceptual Design Optimization of an Augmented Stability Aircraft Incorporating Dynamic Response Performance Constraints", a dissertation submitted to the Graduate Faculty of Auburn University, December 13, 2014
12. Hoe, G., Owens, D.B., and Denham, C., "Forced Oscillation Wind Tunnel Testing for FASER Flight Research Aircraft", American Institute of Aeronautics and Astronautics, Aug 2012
13. Sim, A.G., "Modeling, Simulation, and Flight Characteristics of an Aircraft Designed to Fly at 100,000 Feet", NASA Dryden Flight Research Facility, September 1991.
14. Selig, M.S., Donovan, J.F., and Fraser, D.B., "AIROFOIL AT LOW SPEEDS", H. A. Stokely, publisher, 1989.
15. Schiestel, R., Chaouat, B., "Turbulence modeling and simulation advances in CFD during the past 50 years", Institute du France Academi des sciences, 2022.
16. Hoeger, T.C., "CFD Transient Simulation of an Isolator Shock Train in a Scramjet Engine", Air Force Institute of Technology, July 2012.
17. Soinne, E., "Aerodynamic and Flight Dynamic Simulations of Aileron Characteristics", Department of Aeronautics Royal Institute of Technology Sweden, NOV. 2000.

18. Shawky, A., Aly A.B., Nashar, A., and Elsayed, M., "Hardware-in-the-Loop Simulation for a Small Unmanned Aerial Vehicle", 16th International Conference on AEROSPACE SCIENCES & AVIATION TECHNOLOGY, MAY 2015.
19. Ghika, S.A., and Guerrero, L.A. P., "Mechanical Design, Analysis, and Manufacturing of Wind Tunnel Model and Support Structure", KTH ROYAL INSTITUTE OF TECHNOLOGY, 2021.
20. Saltzman, E.J. and Ayers, T.G., "A Review of flight-To-Wind Tunnel Drag correlation", NASA Dryden Flight research center, November 1, 1981.
21. Weiberg, J.A. and Gamse, B., "LARGE-SCALE WIND-TUNNEL TESTS OF AN AIRPLANE MODEL WITH TWO PROPELLERS AND ROTATING CYLINDER FLAPS", NATIONAL AERONAUTICS AND SPACE ADMINISTRATION, 1968.
22. Koning, W.J.F., "Wind Tunnel Interference Effects on Tilt Rotor Testing Using Computational Fluid Dynamics", Master of Science at the Delft University of Technology, December 18th 2015.
23. Pettersson, K., "Scaling Techniques Using CFD and Wind Tunnel Measurements for use in Aircraft Design", Licentiate Thesis Department of Aeronautical and Vehicle Engineering, Division of Aerodynamics Sweden, September 2006.
24. Greer, H.D., Shivers, J.P., Fink, M.P., Carter, C.R., "WIND- TUNNEL INVESTIGATION OF STATIC LONGITUDINAL AND LATERAL CHARACTERISTICS OF A FULL-SCALE MOCKUP OF A LIGHT SINGLE-ENGINE HIGH-WING AIRPLANE", NATIONAL AERONAUTICS AND SPACE ADMINISTRATION WASHINGTON, D. C, MAY 1973.
25. Matsuo, Y., "Special Contribution Numerical Wind Tunnel: History and Evolution of Supercomputing", Japan Aerospace Exploration Agency, April 2017.
26. Bi, W., Wang, W., Wang, Z., Yunong, "Extending Model-Based Systems Engineering into Integrated Platform Designed for Civil Aircraft Development", São José dos Campos, 2021.
27. Janovec, M., Cernan, J., Novak, A., "Design of construction and instrumentation of the Zlín aircraft simulator", 10th International Conference on Air Transport, 2021.
28. Aati, S. and Nejim, S., "Identification of aircraft aerodynamic derivatives based on photogrammetry and computational fluid dynamics", Journal of Physics, 2019.
29. Ananda, G.K., Vahoray, M., OrDantskerz, D., and Seligx, M.S., "Design Methodology for a Dynamically-Scaled General Aviation Aircraft", 35th AIAA Applied Aerodynamics Conference, June 2017.

30. Vahora, M., Ananday, G.K. , and Seligz, M.S., “Design Methodology for Aerodynamically Scaling of a General Aviation Aircraft Airfoil”, 2018 AIAA Aerospace Sciences Meeting, 2018.
31. Qadri, M., VahoraM. , Hascaryo,R.W. , Finlon,S., Or Dantsker,D., Ananda,G.K., and Selig,M. S., 2018 AIAA Aerospace Sciences Meeting, January 2018.
32. Vahora, M., Ananday, G.K., and Seligz,M.S.,”Design Methodology for Aerodynamically Scaling of a General Aviation Aircraft Airfoil”, Department of Aerospace Engineering, University of Illinois, 2018.